Nonlinear dynamics and two-dimensional solitons for spin-1 ferromagnets with biquadratic exchange

B. A. Ivanov,[1,2,*] A. Yu. Galkin,[3,1] R. S. Khymyn,[2,1] and A. Yu. Merkulov[4]
[1]*Institute of Magnetism, 03142 Kiev, Ukraine*
[2]*National Taras Shevchenko University of Kiev, 03127 Kiev, Ukraine*
[3]*Institute of Metal Physics, 03142 Kiev, Ukraine*
[4]*Macromolecular Ion Physics Group, FOM Institute for Atom and Molecular Physics, Kruislaan 407, 1098 SJ Amsterdam, The Netherlands*
(Received 19 October 2007; published 1 February 2008)

We develop a consistent semiclassical theory of spin dynamics for an isotropic ferromagnet with a spin $S=1$ taking into consideration both bilinear and biquadratic exchange interactions over spin operators. For such non-Heisenberg magnets, a peculiar class of spin oscillations and waves, for which the quantum spin expectation value does not change in direction, but changes in length, is presented. Such "longitudinal" excitations do not exist in regular magnets, the dynamics of which is described in terms of the Landau-Lifshitz equation or by means of the spin Heisenberg Hamiltonian. We demonstrate the presence of nonlinear uniform oscillations and waves as well as self-localized dynamical excitations (solitons) with finite energy. The possibility of excitation of such oscillations by ultrafast laser pulse is discussed.

DOI: 10.1103/PhysRevB.77.064402 PACS number(s): 75.10.Jm, 75.10.Hk, 05.45.Yv

I. INTRODUCTION

Magnetically ordered materials (magnets) are known as essentially nonlinear systems.[1,2] Localized nonlinear excitations with finite energy, or solitons, play an important role in the description of nonlinear dynamics, in particular, spin dynamics for low-dimensional magnets, with a different kind of magnetic order. To date, solitons in Heisenberg ferromagnets, whose dynamics is described by the Landau-Lifshitz equation for the constant-length magnetization vector, have been studied in detail (for a review, see Refs. 2–6). In terms of microscopic spin models, this picture corresponds to the exchange Heisenberg Hamiltonian, with the isotropic bilinear spin interaction $J\mathbf{S}_1\mathbf{S}_2$.[7] For a spin of $S>1/2$, the isotropic interaction is not limited by this term and can include higher invariants such as $(\mathbf{S}_1\mathbf{S}_2)^n$, with n up to $2S$. In particular, the general isotropic model with the spin $S=1$ and the nearest neighbor interaction is described by the Hamiltonian

$$\hat{\mathcal{H}} = -\sum_{\langle i,j\rangle} [J(\mathbf{S}_i\mathbf{S}_j) + K(\mathbf{S}_i\mathbf{S}_j)^2]. \quad (1)$$

Here, the constants J and K determine the spin-bilinear (Heisenberg) and spin-biquadratic exchange interactions between nearest neighbors $\langle i,j\rangle$. This model (1) has been actively studied for the past two decades both in view of description of usual crystalline magnets (see Refs. 8–11 and in application to low-dimensional magnets (see Refs. 12 and 13).

For model (1), the character of the ground state is more complicated than for Heisenberg magnets. It is determined by the values of the parameters of bilinear and quadratic exchange, J and K. In addition to the ferromagnetic phase, which is stable at $J>K$ and $J>0$, and the antiferromagnetic phase, which is stable within the mean field approximation at $J<K$ and $J<0$, two so-called nematic phases (collinear and orthogonal, see Ref. 14) are realized for this model. For these nematic states, the quantum spin expectation value $\mathbf{m}=\langle\mathbf{S}\rangle$ equals zero, even at zero temperature. (Below, for short, we will refer to the vector $\mathbf{m}$ as magnetization.) The areas of existence of the nematic phases separate from both sides the domains of stability for the ferromagnetic and antiferromagnetic phases. Interest in model (1) increases in view of the investigation of multicomponent Bose-Einstein condensates of neutral atoms with nonzero spins.[15] At two chosen values of J/K, namely, at $J=K$ and $J=0$, model (1) has the symmetry SU(3), which is higher than the rotational symmetry inherent to SO(3)$\sim$SU(2) and, in a one-dimensional case, is exactly integrable. The latter is interesting from the theoretical point of view.

A possibility to change the magnetization $\mathbf{m}$ in length is an important peculiarity of the ferromagnetic phase in model (1). It is worth noting that, for the regular Landau-Lifshitz equation, frequently employed for the description of spin dynamics, the magnetization length keeps constant. This property is associated with the fact that the Landau-Lifshitz equations naturally emerge within the approach of spin coherent states, or states of the Lie group SO(3)$\sim$SU(2). They are parametrized by a unit vector; the direction of the latter coincides with the quantum expectation values for the spin operator $\mathbf{m}$, and all quantum expectation values of some products of spin components are expressed through corresponding products of expectation values for components of spin operators (dipolar variables) (for a review, see Refs. 16 and 17).

For a Heisenberg ferromagnet with a purely bilinear exchange ($K=0$), the approach based on SO(3)—coherent states—is exact, whereas for model (1) one has to take into consideration quantum expectation values for all irreducible operators, which include not only dipolar variables $\mathbf{m}$, but also so-called quadrupolar variables, bilinear on components of spin operator $\mathbf{S}$. In principle, such variables cannot be reduced to $\mathbf{m}$ only; for example, $\langle S_x^2 - S_y^2\rangle$ can be nonzero even with the values $\langle S_x\rangle=0$ and $\langle S_y\rangle=0$. In fact, Hamilton dynamics of the variable $m=|\mathbf{m}|$ takes place, and a variable,

canonically conjugated to m, is a quadrupolar variable of a structure mentioned above. Such dynamics, which is appropriately called *longitudinal*, in principle, does not exist for a Heisenberg ferromagnet while considered within the framework of the Landau-Lifshitz equation or the Hamiltonian (1) with $K=0$.

The fast change of the length of the magnetization $\mathbf{m}$ is of great interest now. Thermal quenching of magnetization length, caused by ultrafast (femtosecond) laser pulse, is known for different ferromagnets for nearly ten years.[18–20] Nonthermal laser control of magnetization is also realized[21,22] (for a review, see Ref. 23). Principal possibility of dynamical (besides heating) quenching of $m=|\mathbf{m}|$ up to the values $m\approx 0$ and ultrafast dynamics of the variable m is of great scientific and technological interest.

For model (1), one-dimensional (1D) solitons[24] and two-dimensional (2D) topological solitons in the collinear nematic phase,[12,25] and near the SU(3)-symmetrical point,[26] have been studied. However, nonlinear dynamics for other phases, even for the simplest ferromagnet phase, has not been studied yet. In this work, we investigate 2D longitudinal nonlinear spin oscillations and solitons in the ferromagnetic phase of a non-Heisenberg ferromagnet within a consistent semiclassical description of model (1). In Sec. II, the equations for a full set of spin quantum expectation values obtained within semiclassical approximation and describing the effects of dynamical quantum spin reduction are discussed. Nonlinear longitudinal spin oscillations in such a system are found there. Interaction of corresponding nondipolar degrees of freedom with electromagnetic field is also discussed in this section.

In the next sections, we demonstrated the presence of specific *longitudinal solitons*, in which the direction of the magnetization vector $\mathbf{m}$ remains constant, but the magnetization changes in length. Such soliton solutions are obtained in the framework of the semiclassical equations, in a continual approximation (Sec. III), and by analyzing a discrete problem for a simple square lattice (Sec. IV). Section V contains conclusions and discussions of results obtained, as well as some overview of the open problem. The discussion of the possibility of excitation of longitudinal spin oscillations by ultrashort laser pulse is also present in Sec. V.

II. MODEL AND ELEMENTARY EXCITATIONS

To develop a semiclassical theory describing a magnet with a spin $S=1$ with Hamiltonian (1) and to make allowance for the spin reduction on a lattice site, we introduce generalized coherent states of SU(3) group parametrized by a three-dimensional complex vector $\mathbf{u}+i\mathbf{v}$, (see Refs. 12 and 26),

$$|\mathbf{u},\mathbf{v}\rangle = \sum_{j=x,y,z} (u_j + iv_j)|t_j\rangle, \tag{2}$$

where $|t_j\rangle$ are three Cartesian states for spin $S=1$, and $\mathbf{u}$ and $\mathbf{v}$ are real vectors. With account taken of the normalization requirements and arbitrariness of the total phase, the vectors $\mathbf{u}$ and $\mathbf{v}$ satisfy the conditions

$$\mathbf{u}^2 + \mathbf{v}^2 = 1, \quad \mathbf{uv} = 0. \tag{3}$$

In terms of the variables $\mathbf{u}$ and $\mathbf{v}$, all irreducible quantum expectation values for spin $S=1$ states, including the magnetization vector $\langle \mathbf{S}\rangle = \mathbf{m}$ and quadrupolar variables $\langle S_iS_j + S_jS_i\rangle$, can be expressed by the simple relations

$$\mathbf{m} = 2(\mathbf{u}\times\mathbf{v}), \quad \langle S_iS_k + S_kS_i\rangle = 2(\delta_{ik} - u_iu_k - v_iv_k). \tag{4}$$

For the ferromagnetic ground state, which is stable for $J > K$ and $J>0$, the value of $|\mathbf{m}|=1$, while the state is degenerated in the direction of $\mathbf{m}$. It means that in the ground state, $|\mathbf{u}|=1/\sqrt{2}$ and $|\mathbf{v}|=1/\sqrt{2}$. At $|\mathbf{m}|=1$, rotation of these vectors in a plane perpendicular to $\mathbf{m}$ does not change the state of a system. However, for any $|\mathbf{m}|<1$, states which differ from each other by the direction of $\mathbf{u}$ and $\mathbf{v}$ in the plane are physically distinguished due to anisotropy of quadrupolar variables. As we will see below, the angle of rotation of $\mathbf{u}$ and $\mathbf{v}$ plays the role of a generalized coordinate conjugated to the magnetization length $m=\mathbf{m}$.

Dynamics of the variables $\mathbf{u}$ and $\mathbf{v}$ for a given spin on a point i in a lattice is determined by a Lagrangian,[12]

$$L = -2\hbar\sum_i \mathbf{v}_i(\partial\mathbf{u}_i/\partial t) - W\{\mathbf{u},\mathbf{v}\}, \tag{5}$$

where $W\{\mathbf{u},\mathbf{v}\}$ is the system energy, which coincides with the quantum expectation value of the Hamiltonian (1) calculated with the coherent states (2). For a lattice discrete model, an expression for the energy $W\{\mathbf{u},\mathbf{v}\}$ is given in Ref. 12. Based on this Lagrangian, we can easily analyze both the linear and nonlinear dynamics of the ferromagnet. In particular, using the explicit form of the energy $W\{\mathbf{u},\mathbf{v}\}$ proposed in Ref. 12, we can readily obtain the spectrum of linear elementary excitations (magnons). This spectrum contains two modes. The first mode does not depend on the biquadratic interaction constant K. Its dispersion relation has the same form as for the usual Heisenberg ferromagnet, $\varepsilon(\mathbf{k})=4J[1-C(\mathbf{k})]$, where $C(\mathbf{k})=(1/2)[\cos(k_xa)+\cos(k_ya)]$, $\mathbf{k}=\mathbf{p}/\hbar$, $\mathbf{p}$ is the magnon momentum, and a is the lattice constant (below, we will limit ourselves to a two-dimensional square lattice). In the long-wave limit, $ka\ll 1$, $k=|\mathbf{k}|$, the usual parabolic dispersion law appears, $\varepsilon\simeq J(ka)^2$. The second mode describes the oscillations of the modulus of magnetization, $m=|\mathbf{m}|$, coupled with some quadrupolar variables. It is natural to call them *longitudinal magnons* [see Eqs. (9) and (10) below].

It is difficult to analyze the nonlinear dynamics of the variables $\mathbf{u}$ and $\mathbf{v}$ since we have to operate with four independent nonlinear equations rather than with two equations for angular variables, as in the case of the usual ferromagnet. However, it is possible to show that the full set of nonlinear equations for the $\mathbf{u}$ and $\mathbf{v}$ vectors has a partial planar solution, for which the magnetization vector changes its length only, $\mathbf{m}=m\mathbf{e}_3$, and vectors $\mathbf{u}$ and $\mathbf{v}$ rotate in the perpendicular plane (1, 2), where $\mathbf{e}_1$ and $\mathbf{e}_2$ are unit vectors in the plane, perpendicular to the magnetization vector $\mathbf{m}=m\mathbf{e}_3$, and $\mathbf{e}_i$, $i=1$ 2, and 3, present an orthogonal set of unit vectors. Below, we will restrict ourselves to the analysis of such planar solutions. For this solution, only three quantum expectation values are nontrivial, namely, the magnetization $\sigma_3=m=2(u_1v_2-u_2v_1)$ and two quadrupolar variables, $\sigma_1=\langle S_1^2-S_2^2\rangle$

$=u_1^2-u_2^2+v_1^2-v_2^2$ and $\sigma_2=\langle S_1S_2+S_2S_1\rangle=-2u_1u_2-2v_1v_2$. One can easily show that $\sigma_1^2+\sigma_2^2+\sigma_3^2=1$; that is, the vector $\boldsymbol{\sigma}=\sigma_1\mathbf{e}_1+\sigma_2\mathbf{e}_2+\sigma_3\mathbf{e}_3$ is a unit vector. It is convenient to introduce the angular representation for this unit vector,

$$\sigma_3=\cos\,\theta,\quad \sigma_1=\langle S_x^2-S_x^2\rangle=\sin\,\theta\cos\,\phi,$$

$$\sigma_2=\langle S_xS_y+S_yS_x\rangle=\sin\,\theta\sin\,\phi. \tag{6}$$

The advantage of these variables is that they are unambiguously determined from a given physical state of the system. In contrast, the variables $\mathbf{u}$ and $\mathbf{v}$ contain the halved values of the angular variables θ and ϕ that reflects the nature of vector $\mathbf{u}$ (or $\mathbf{v}$) as a vector—director. Using the angular variables θ and ϕ, we can reduce the Lagrangian (5) to the form

$$\mathcal{L}=\frac{\hbar}{2}\sum_i(\cos\,\theta_i-1)\left(\frac{\partial\phi_i}{\partial t}\right)-W\{\theta,\phi\}, \tag{7}$$

where $W\{\theta,\phi\}$ is the system energy, which depends on the discrete variables θ_i and ϕ_i. It is convenient to present the energy through the vector variable $\boldsymbol{\sigma}$,

$$W=-\frac{1}{2}\sum_{\langle i,j\rangle}[K\boldsymbol{\sigma}_i\boldsymbol{\sigma}_j+2(J-K)\sigma_{i,3}\sigma_{j,3}]. \tag{8}$$

It is interesting to note that this Lagrangian formally coincides with that for a spin $S=1/2$ uniaxial ferromagnet which is known as the XXZ model. For this model, the constant of isotropic exchange is equal to $K/2$, and anisotropy of spin interaction is proportional to $J-K$. Thus, the general dynamics of SU(3)-coherent state for spin-1 magnet includes the particular class of solutions which is described by a *classical* model for a spin $S=1/2$, which is quite an unusual model for the theory of magnetism. Limit cases correspond to the following simple physical models: in the vicinity of a transition to the nematic phase, SU(3)-symmetrical point $K\to J$, an effective spin model (8) becomes isotropic, while at $K/J\to 0$, we arrive at the Ising model. Naturally, anisotropy of the effective model is realized in the $\boldsymbol{\sigma}$ space and has no direct linkage to spacious rotations of spin operators.

For model (7), it is easy to obtain oscillations, which are a nonlinear analogy of the above mentioned longitudinal magnons. For this excited states, at the lattice site $\mathbf{l}_i$, the variable $\theta_i=\theta_0=$const does not depend on time and $\phi_i=\mathbf{kl}_i+\omega t$. The frequency of such oscillations ω depends on the wave vector $\mathbf{k}$ and the amplitude θ_0 as follows:

$$\omega(\mathbf{k})=(4\cos\,\theta_0/\hbar)\{2(J-K)+K[1-C(\mathbf{k})]\}. \tag{9}$$

Within the linear approximation, at $\theta_0\to 0$, this frequency becomes the frequency of longitudinal magnons, previously obtained by Papanicolaou.[27] In the long-wave limit, this spectrum becomes parabolic, and can be written as

$$\omega(\mathbf{k})=\omega_0\cos\,\theta_0(1+r_0^2k^2), \tag{10}$$

where

$$\hbar\omega_0=8(J-K),\quad r_0^2=Ka^2/8(J-K). \tag{11}$$

Here, the frequency ω_0 is a gap of longitudinal magnons and r_0 determines a characteristic space scale. A study based on the Lighthill criterion, see, for example, Ref. 28, shows that such uniform oscillations being excited in the system (for example, by ultrafast laser pulse, see below) are unstable against self-focusing. As a result, essentially nonuniform states, like solitons, should appear. For their analysis, it is easier to employ a continual approximation, considering θ_i and ϕ_i to be continuous functions of coordinates and time, $\theta_i(t)\to\theta(\mathbf{x},t)$ and $\phi_i(t)\to\phi(\mathbf{x},t)$. For a 2D system, or for a thin enough film of magnet, which complies with standard geometry of experiment,[23] one can use 2D solutions and present the Lagrangian of the problem as $\mathcal{L}=\int L\{\theta,\phi\}d^2x$, where the density of the Lagrangian is

$$L=(\hbar/2a^2)(\cos\,\theta-1)(\partial\phi/\partial t)-w\{\theta,\phi\}, \tag{12}$$

and the energy density $w\{\theta,\phi\}$ is determined by the formula

$$w\{\theta,\phi\}=(2/a^2)(J-K)\sin^2\,\theta+(1/4)K\sin^2\,\theta(\nabla\phi)^2+(1/4)[K+2(J-K)\sin^2\,\theta](\nabla\theta)^2. \tag{13}$$

As we will see below, solitons exist at $0<K<J$, and we will limit ourselves to this region of the parameters.

Let us discuss briefly an interaction of longitudinal degrees of freedom with external fields, having in mind primarily the possibility of experimental excitation of such oscillations. First of all, a magnetic field $\mathbf{H}=H\mathbf{e}$ affects only the magnetization; for a planar solution, it is $\mathbf{m}=\langle\mathbf{S}\rangle=\mathbf{e}_3\cdot\cos\,\theta$. Therefore, Zeeman interaction of $\boldsymbol{\sigma}$ with the magnetic field parallel to some direction $\mathbf{e}$ is described by the Hamiltonian $H^H=-H(\mathbf{e},\mathbf{e}_3)\sigma_3$. Actually, the magnetic field directed parallel to the mean spin $\mathbf{m}=\langle\mathbf{S}\rangle$ does not affect the system state, while for any other directions of $\mathbf{H}$, one can expect a trivial change of the orientation of unit vectors $\mathbf{e}_i$ describing the planar solution. It turns out that ac-magnetic field is not effective for excitation of longitudinal oscillations.

It appears that excitation of longitudinal oscillations may be done through the application of an electric field on the system. For simplicity, we will start with dc-electric field. Interaction of such electric field with a spin system of a magnet can be described phenomenologically on the basis of the following Hamiltonian:

$$H^{(int)}=\frac{1}{8\pi}\varepsilon_{ij}^{(\mathrm{spin})}E_iE_j, \tag{14}$$

where $\varepsilon_{ij}^{(\mathrm{spin})}$ is a spin-dependent part of dielectric permittivity and $\mathbf{E}=E\mathbf{e}$ is the electric field, where $\mathbf{e}^2=1$ (see Ref. 29). In principle, $\varepsilon_{ij}^{(\mathrm{spin})}$ can include all spin variables describing the system state and allowed by symmetry.[30,31] In our case, the components of $\varepsilon_{ij}^{(\mathrm{spin})}$ should include the contribution from quadrupolar variables, $\varepsilon_{ij}^{(\mathrm{spin})}E_iE_j=\varepsilon^Q\langle S_iS_j+S_jS_i\rangle E_iE_j$. The discussion of the microscopic origin of such interaction, in particular, the value of the constant ε^Q, is far from the scope of this paper.

A possible role of quadrupolar interactions can be demonstrated by a simple example. Consider an electric field perpendicular to the magnetization in the ground state $\mathbf{m}=m\mathbf{e}_3$. It can be easily seen that the influence of such field is equivalent to the action of some "effective field" $\mathbf{H}^Q$ on the variable $\boldsymbol{\sigma}$ of the same form as the Zeeman interaction of the usual magnetic field with the usual magnetic moment, $H^{(\mathrm{int})}=-\mathbf{H}^Q\boldsymbol{\sigma}$. Here, the effective field $\mathbf{H}^Q$ is described by

$$\mathbf{H}^Q = \frac{\varepsilon^Q}{8\pi}\{[(\mathbf{e}_1,\mathbf{E})^2-(\mathbf{e}_2,\mathbf{E})^2]\mathbf{e}_1+2(\mathbf{e}_1,\mathbf{E})(\mathbf{e}_2,\mathbf{E})\mathbf{e}_2\} = \frac{\varepsilon^Q E^2}{8\pi}(\mathbf{e}_1\cos\alpha+\mathbf{e}_2\sin\alpha), \tag{15}$$

where α is a doubled value of the angle between the vector of electric field $\mathbf{E}$ and the direction of unit vector $\mathbf{e}_1$ in planar solution. Then a simple analogy between the action of the usual magnetic field $\mathbf{H}$ on the magnetization $\mathbf{m}$ and the action of the field $\mathbf{H}^Q$ on the vector $\boldsymbol{\sigma}$ becomes obvious.

For consideration of ac field, for example, the electric field of electromagnetic wave (light), it is enough to replace $(1/8\pi)E_iE_j$ by $(1/16\pi)E_iE_j^*$, where E_i now is the complex amplitude of the time-dependent electric field.[29] For linearly polarized light, the same expression (15) for the effective field appears. If light intensity is time dependent, for example, for modulated laser beam or for ultrashort laser pulse, the effective field $\mathbf{H}^Q$ will be time dependent. Being linearly coupled with variables σ_1 and σ_2, it can excite the longitudinal spin oscillations found above.

III. LONGITUDINAL SOLITONS IN A CONTINUAL MODEL OF A MAGNET

As the Lagrangian does not depend directly on ϕ, but on its derivatives, the models (12) and (13) have an integral of motion, which determines the total spin projection on some axes. The same integral of motion is present for discrete models (7) and (8). This integral of motion is suitable to be presented via the number of spin deviations in the system N; for the discrete model and its continuous counterpart, it reads

$$N=\sum_i(1-\cos\theta_i) \quad \text{or} \quad N=\int(1-\cos\theta)d^2x/a^2. \tag{16}$$

In the framework of quantum mechanics, N possesses integer values and, in line with Ref. 3, we use this quantity for semiclassical quantization of solitons. The important integral of motion is soliton energy E [Eq. (8)] which, within the continuous approximation, turns into $E=\int w\{\theta,\phi\}d^2x$.

The integral of motion (16) results in solutions with stationary dynamics, for which the vectors $\mathbf{u}$ and $\mathbf{v}$, as well as in-plane components of the vector $\boldsymbol{\sigma}$, rotate in the plane (1, 2) with some constant frequency. In this case, the variable θ depends only on the distance from a certain point in the plane, which is considered as the center of a soliton. We limit ourselves to the analysis of these solutions based on ansatz of the form

$$\theta=\theta(r), \quad \varphi=\omega t, \quad r=|\mathbf{x}|. \tag{17}$$

Such solitons formally resemble so-called precessional solitons, which are known for the case of uniaxial Heisenberg ferromagnets with precession of a unit vector of magnetization $\mathbf{m}$, $|\mathbf{m}|=1$, around an easy axis (z axis) with a constant frequency ω_H and with an amplitude $m_\perp=\sin\vartheta(r)$ depending on r, $\vartheta(r)\to 0$ at $r\to\infty$ (for a review, see Ref. 3). In spite of the principal difference in the physical properties of these two types of solitons, many of their formal features are similar. The latter allows us not to discuss some details.

The function $\theta(r)$ is determined by an ordinary differential equation,

$$\left(\theta''+\frac{\theta'}{r}\right)\left(r_0^2+\frac{a^2}{4}\sin^2\theta\right)+\frac{\omega}{\omega_0}\sin\theta-\sin\theta\cos\theta\left(1-\frac{\theta'^2a^2}{4}\right)=0, \tag{18}$$

where the prime denotes the derivative over r, and the characteristic size r_0 and the magnon gap frequency ω_0 are determined above [Eq. (11)]. Far from a soliton, the state should correspond to the ground state of the system, i.e., the condition $\theta(r)\to 0$ at $r\to\infty$ should be fulfilled. The condition $\theta'(0)=0$ ensures the absence of singularity at $r=0$. Equation (18) with such boundary conditions can be easily solved by the "shooting" method.[3] It has a discrete set of solutions $\theta=\theta_n(r)$ with n nodes at points $r=r_n\neq 0$, $n=1,2,\ldots$. Solitons with nodes are unstable,[3] and we will discuss the solution with $n=0$ and a monotonous decay of the function $\theta(r)$ only.

Knowing the solution of $\theta(r)$, one can calculate integrals describing E and N, and represent the soliton energy as a function of the number of magnons bounded in the soliton, $E=E(N)$. As already mentioned, this procedure at $N\gg 1$ and within the continual approximation is equivalent to a semiclassical quantization of solitons (for the discrete model, some peculiarities occur; see Sec. V). It is convenient to use the fact that Eq. (18) can be formally obtained from variation of the functional $\tilde{\mathcal{L}}=E-\hbar\omega N$, $\delta\tilde{\mathcal{L}}/\delta\theta=0$. The functional $\tilde{\mathcal{L}}$ coincides with Lagrangian (5) calculated within the ansatz (17). The condition $\delta\tilde{\mathcal{L}}/\delta\theta$ immediately leads to the relation

$$\hbar\omega=dE(N)/dN, \tag{19}$$

which coincides with that for precessional solitons. Equation (19) describes the quantum sense of the classical parameter ω in the solution of the form (17): the value of $\hbar\omega$ at $N\to\infty$ is equal to a change of the soliton energy with a change of the number of bound magnons by 1.

Some limit characteristics of solitons can be obtained without an exact solution of Eq. (18). Using the phase plane method, it is easy to demonstrate that a soliton solution exists only at $0<\omega<\omega_0$ and its characteristics depend on the parameter ω/ω_0. At $(1-\omega/\omega_0)\ll 1$, the soliton amplitude is small and the function $\theta(r)$ takes the form

$$\theta(r)=\sqrt{1-\omega/\omega_0}f[(r/r_0)\sqrt{1-\omega/\omega_0}], \tag{20}$$

where $f(x)$ is a universal function, localized in the area of $\Delta x\sim 1$ with the value of the order of 1 at the origin. Further,

it is possible to demonstrate that for all K/J at $\omega \to \omega_0$, soliton energy tends to a finite value $E \to E_0 = \eta \cdot 4\pi K$, where $\eta \approx 0.93$ is a numerical coefficient. In this limit, the number of magnons is also finite, $N \to N_{\min} = 2\eta N_2$, where $N_2 = 2\pi(r_0/a)^2$ is the characteristic number of magnons.

These values are minimal for solitons in a magnet with a given parameter K/J, and in the limit $\omega \to \omega_0$, the connection $E \to \hbar\omega_0 N$, which is typical for linear theory, appears. A similar property takes place for a precessional soliton with small amplitude,[32] with an essential difference, such that for a precessional soliton the value of E_0 is always of the order of the exchange integral J and can be compared with the energy of a Belavin-Polyakov (BP) topological soliton $E_{BP} = 4\pi J$, whereas for a longitudinal soliton for small K/J, the inequality $E_0 \ll E_{BP}$ formally may be realized. In fact, for $K \ll J$, the continual approximation fails even at $N \sim 1$, and the minimal value of soliton energy E cannot be smaller than $2.57J$ (see the last paragraph of the next section). On the other hand, the value of E_0 found here within the continual approximation is valid for a wide region of parameters like $0.7J < K < J$, where the value of $N_{\min}$ is larger than 4 (see the next section).

Another limit case corresponds to the condition $0 < \omega \ll \omega_0$. To discuss it, we mention that for $\omega = 0$, the 2D soliton solution is absent; however, equations allow a 1D longitudinal domain-wall-like solution. For this solution, $\mathbf{m}(\xi) = m(\xi)\mathbf{e}_3$, with $m(\xi) \to 1$ at $\xi \to \infty$ and $m(\xi) \to -1$ at $\xi \to -\infty$; ξ is a coordinate along some direction in the magnet's plane. This wall has a characteristic width of the order of r_0 and energy $\sigma = \sigma(K,J)$ per unit length. A qualitative analysis of Eq. (18) shows that, at $0 < \omega \ll \omega_0$, a soliton contains a large enough circular region with a radius $R \gg r_0$ separated from the rest of the magnet by such a wall. Here, again, the situation is common for precessional solitons.[3]

Further, it is easy to obtain a qualitative description of a soliton in this limit case. Apparently, the fact that a uniform state with $m(\xi) = -1$ has the same energy as that with $m(\xi) = 1$, and a finite region with $m(\xi) = -1$, i.e., $\theta = \pi$, does not contribute to energy, but affects the value of N. In this case, energy loss is connected only with the presence of a domain wall separating the inner region from the rest of the magnet. For the circular area, energy loss is minimal at a given N and one can see that $N = 2\pi R^2$ and $E = 2\pi\sigma R$, where R is the radius of this area. Proceeding from that, one can obtain a square root dependence of soliton energy on the number of bounded magnons N for a large soliton radius, which corresponds to the condition $N \gg N_2$,

$$E = a\sigma\sqrt{2\pi N}. \tag{21}$$

Thus, in the limit cases, the dependence of soliton energy on N, and also on the parameters J and K, is easily reconstructed. In the intermediate frequency range, which corresponds to numbers of magnons N of the order of a few $N_{\min}$, a thorough analysis of Eq. (18) is needed. We carried numerical calculations for a set of values of K/J for the region of interest $0 < K < J$. The analysis was done as follows: at the given K/J, Eq. (18) was solved numerically for a set of values of ω/ω_0 which were chosen with different steps. Further, having a solution, the value of energy E and the number of magnons N were calculated. Then the dependencies $E(N)$ and $\omega(N)$ [the latter is important for the analysis of stability of a soliton, which is stable in continual model at $d\omega(N)/dN > 0$ only] were constructed.

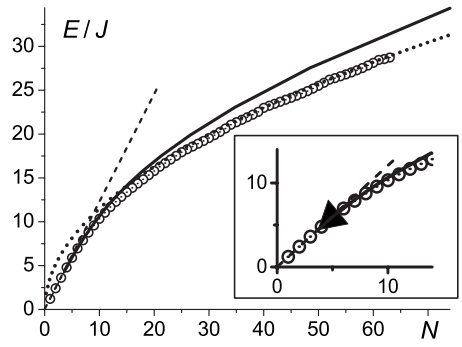

FIG. 1. The soliton energy E (in the unit of the exchange integral J) dependence on the number of magnons N for the case $K = 0.7J$. The results of the continual approximation are represented by the solid line; the symbols are results of a numerical analysis of the discrete model (see the next section). In the inset, details of the behavior at small N are present; the arrow's end points out the end point of the dependence $E(N)$, i.e., minimal value of soliton energy. The symbols beneath the arrow depict delocalized magnon states found by numerical simulation for a finite system. The dash line and dotted line represent asymptotic behaviors at $E \to \hbar\omega_0 N$ and square root asymptotic (19) for small and large N, respectively.

Let us briefly discuss the main characteristics of solitons found within continual approximation. The analysis confirmed asymptotic dependencies derived above (see Figs. 1 and 2). In the whole region of parameters of the problem, the function $\omega(N)$ monotonously decreases with N growth, i.e., the stability condition is fulfilled. Thus, in the framework of the continual approximation, stable soliton solutions exist within the parameter region $0 < K < J$ of Hamiltonian (1). The soliton energies have a lower limit, E_0, which is smaller than the energy of familiar Belavin-Polyakov solitons.

IV. DISCRETENESS EFFECTS FOR LONGITUDINAL SOLITONS

Strictly speaking, the continual approximation is valid only when the characteristic size of a soliton is essentially

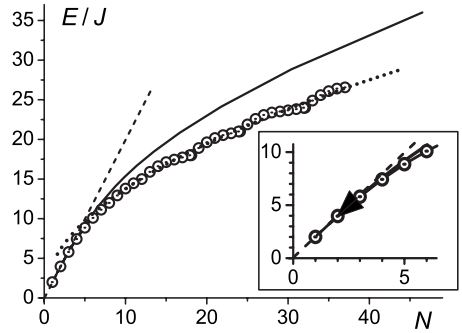

FIG. 2. The same as in Fig. 1, but for the case $K = 0.5J$. Please note essentially smaller values of $N_{\min}$ and E_0.

bigger than the interatomic distance, $|\nabla\theta| \ll 1/a$. This condition may be met for solitons with small amplitude [see Eq. (20)], and also in the limit case $J-K \ll K$, when the characteristic size r_0 is larger than the lattice constant a, $r_0 \gg a$. However, in contrast to precessional solitons in Heisenberg magnets with weak anisotropy, in which the characteristic length is from tens to hundreds of lattice constant, in our case the condition $r_0 \gg a$ is much stricter. Even for enough small $J-K=0.1J$, the value $r_0=1.095a$ only slightly exceeds the lattice constant a. In the region of the parameters $K \sim J-K \sim J$ and in the especially interesting case $K \ll J$, when the minimal energy of solitons is small, an applicability of this approach is not clear and one can expect essential discreteness effects.

Let us consider the discrete models (7) and (8) for a square lattice. Analysis of discrete equations for the variables θ_i and ϕ_i given for each lattice site demonstrates existence of a solution in the form of $\varphi_i=\omega t$ and, further, it is possible to study only variables θ_i.

For the analysis of solitons, we employ the variation procedure proposed and numerically realized in Ref. 33. We will seek a conditional minimum of Hamiltonian, in fact, classical energy $W(\theta_i)$, with respect to variables θ_i, under the condition that the number of magnons $N=\Sigma_i(1-\cos\theta_i)$ is fixed. While seeking a minimum, one can find the precession frequency ω from the equation $\partial W/\partial\theta_i=\hbar\omega\sin\theta_i$. It is worth noting that the sign of derivative $d\omega/dN$ in a discrete case is not important; a soliton is stable if the found conditional extreme of energy is minimum. Analysis was done for an approximately circular fragment cut from a square lattice sized 24×24. We limit ourselves to such size as states we are interested in are essentially localized, and the influence of borders on them is negligible, while the increase of a sample size requires a significant increase of numerical calculation time. As one can expect, at small values of $(J-K)/K$, the behavior of the dependencies $E(N)$ and $\omega(N)$ merely follows curves obtained within the continual approximation, therefore we do not present them. Similarly, for a region of small N, our analysis demonstrates that even in the case $r_0 \leqslant a$ the results of the continual approximation are quite close to numerical data (see Figs. 1 and 2).

It is interesting to note that even for large N, when the characteristic size of inhomogeneity in a solution is of the order of $r_0 < a$, these results qualitatively describe the dependence $E(N)$ even at moderate values of K/J, such as $K/J=0.7$ and $K/J=0.5$, for which $r_0=0.54a$ and $r_0=0.354a$, respectively. For $K/J=0.7$, numerical data adhere closely to continual curves, and a square root dependence with fitted value of domain wall energy σ is working rather well. Even for the smaller value $K/J=0.5$, only insignificant sign-alternating deviations from the square root dependence (21), which are almost invisible in Fig. 1 for $K/J=0.7$, are observed on the numerical data in Fig. 2.

However, apart from such characteristic of a soliton as $E(N)$, which depends on integral values E and N only, effects of discreteness, nevertheless, are essential. This is apparently demonstrated in the dependence $\omega(N)$ (see Figs. 3 and 4) and especially it is clearly seen in the analysis of the soliton structure, i.e., real distribution θ_i in the lattice (see below).

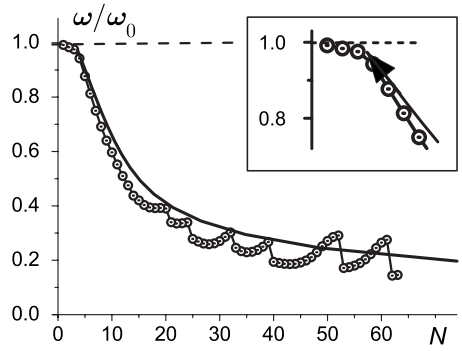

FIG. 3. The dependence of the oscillation frequency ω (in ω_0 units) on the number of magnons N for a soliton in the case $K=0.7J$. The results of the continual approximation are shown by the solid line; symbols are a result of the numerical analysis of the discrete model. The horizontal dash line points out the theoretical value of magnon gap ω_0. In the inset, details of the behavior at small N are shown; the end of the arrow points out to the end point of continual dependence $N=N_{\min}$. Symbols on the left side of the arrow correspond to delocalized magnon states, their insignificant deviations from the value of ω_0 are caused by boundary effects, naturally present for a finite system.

For dependencies $\omega(N)$ when N grows at the beginning, at small N, regular deviation of numerical data from the continual curve is observed. This feature can be explained by the fact that $\omega \propto dE/dN$, whereas the energy $E(N)$ in the discrete model is lower than in continuum. However, even for $K/J=0.7$, noticeable deviations up and down from the smooth dependence typical for continual approximation were observed (see Fig. 3). For smaller value $K/J=0.5$, this irregular behavior is much more essential (see Fig. 4). This complicated behavior is observed in that region of $N > 10 \gg N_{\min}$, where the effective domain wall approximation and the square root asymptotic (21) should be applicable. Therefore, as for precessional solitons in a Heisenberg magnet with strong single-ion anisotropy,[33] it can be naturally associated with characteristics of lattice pinning of a domain wall. Let us discuss the structure of a soliton for $K/J=0.5$ (see Figs. 5 and 6).

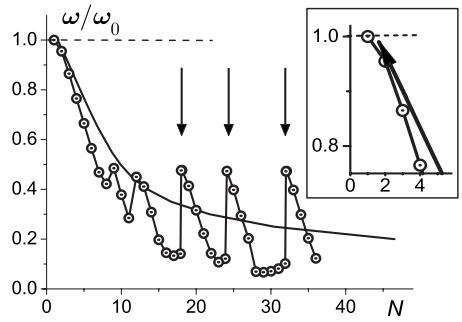

FIG. 4. The same as in Fig. 3, but for the case $K=0.5J$. The vertical arrows denote special values of $N=18$, 24, and 32 (see the text). Please note that the dependencies correspond to each other even at not small $(\omega-\omega_0)/\omega_0 \leqslant 0.25$, which corresponds to $N \leqslant 5$. It is worthly to mention that only one nonlocalized state with $N=1$ was revealed.

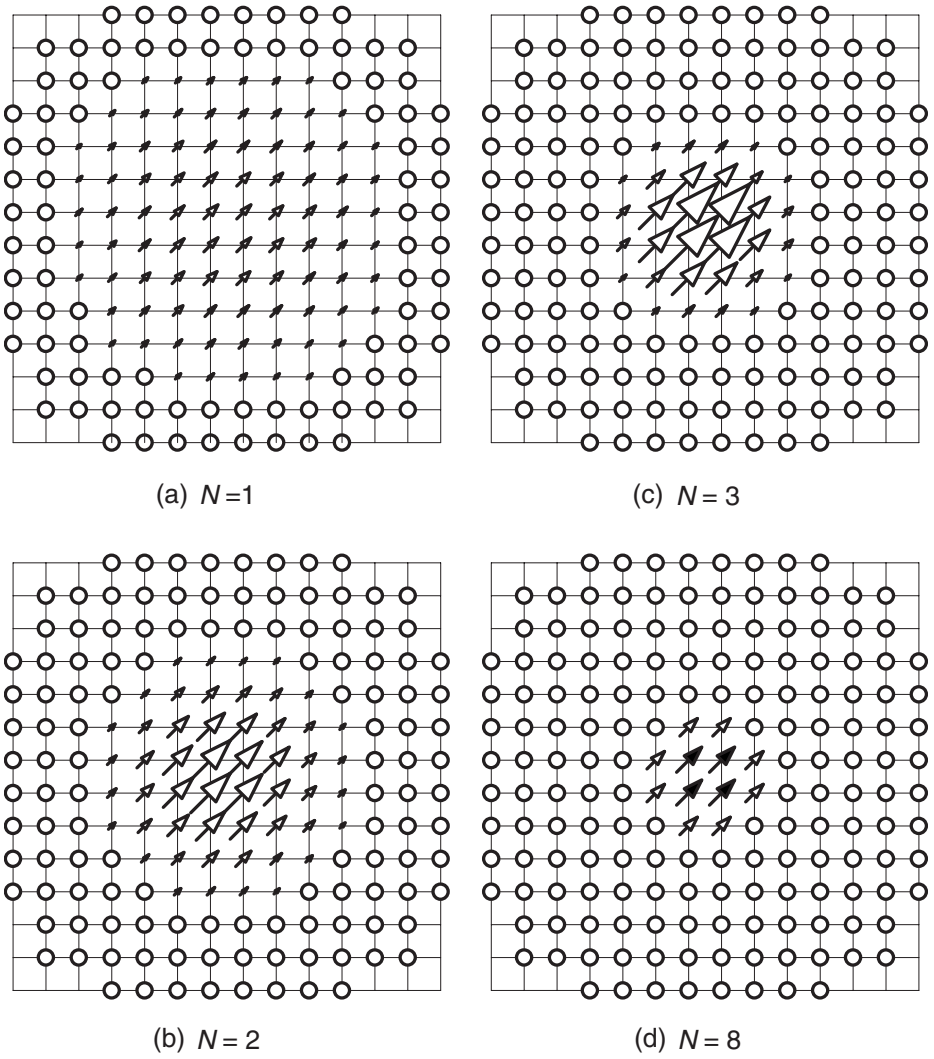

FIG. 5. Distribution of the discrete variables θ_i and ϕ_i in a soliton at small N for the system with $K/J=0.5$. Only a small part of fragment chosen for numerical calculation is presented. θ and ϕ for each spin are presented in the form of 3D vector $\boldsymbol{\sigma}=(\sin\theta\cos\phi, \sin\theta\sin\phi, \cos\theta)$. Values of $5° < \theta_i \leqslant 90°$ are presented by arrows with open heads, while for $90° < \theta_i < 180°$ by arrows with solid heads; the small values $0 \leqslant \theta_i < 5°$ are presented by open circles. The transition from nonlocalized state at $N=1$ to localized states at $N>1$ is clearly seen. For $N=3$, the minimal value of $|\mathbf{m}|=|\cos\theta| \approx 0.5$ is observed in the soliton center. For $N=8$, the values of θ_i near the soliton center are 158° and 15°, and the tendency of transition to collinear structure is seen.

At small N, numerical analysis demonstrates almost radially symmetric distribution of θ_i with the scale of a few lattice constant a, which is essentially larger than $r_0=0.354a$. It is interesting to note that even such a sensitive parameter as the minimal value of N is well reproduced by the continual calculation. According to our continuum calculation, for a magnet with $K/J=0.5$, the value $N_{\min}=1.6$. The discrete analysis provides good localization of a soliton at $N=2$ and 3, and much less localized state at $N=1$ (see Fig. 5). With further growth of N up to $N \leqslant 10$, the distributions of θ_i become sharper and tendency of formation of collinear states is observed. For the values of $N \geqslant 10$, the role of discreteness effects, primarily effects of domain wall pining, increases. This pinning may include either the dependence of the wall energy on its orientation related to lattice vectors or the dependence of the wall energy on its position related to distance to corresponding atomic lines in the lattice.

A set of our numerical results may be explained considering that, like in the case of uniaxial Heisenberg ferromagnet (see Ref. 33), the most favorable position for a domain wall is to be placed between atomic lines like (0,1) or (1,0), but in contrast to Ref. 33, the domain wall is quite flexible and its bend from the line (0,1) to (1,0) does not cost too much energy. In principle, it corresponds to the conclusions of Gochev,[34] who has demonstrated that for a 2D discrete classical spin model with anisotropy like Eq. (8), pinning effects are present for a domain wall parallel to the axes (0,1) and (1,0), and are absent for a wall parallel to atomic lines like (1,1). On the basis of these assumptions, one can describe the real distribution of the θ_i amplitude and the complicated behavior of $\omega(N)$ in a lattice soliton.

In the case $r_0 \leqslant a$, the favorable wall placed between adjacent lines like (0,1) or (1,0) is nearly collinear. Therefore, the most favorable values of N are those for which a soliton

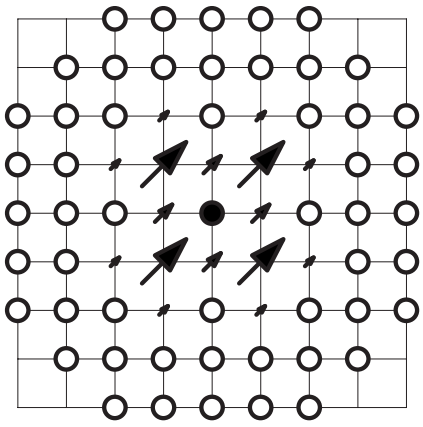

(a) $N=17$

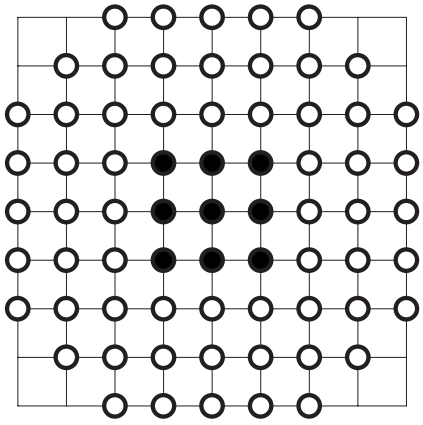

(b) $N=18$

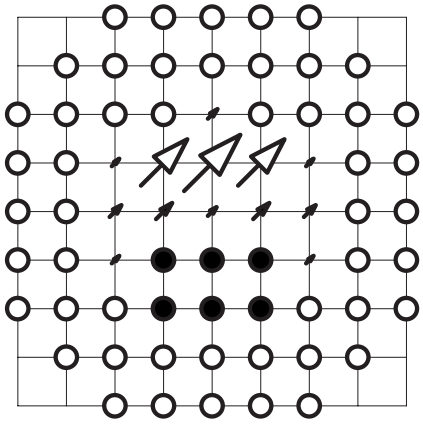

(c) $N=19$

FIG. 6. The distribution of the discrete variables θ_i for a soliton for $K/J=0.5$ at values of N close to magic value $N=18$. Values $0 \leqslant \theta_i < 5°$ and $175° < \theta_i \leqslant 180°$, corresponding to nearly maximal value of spin along the directions up and down, presented by open and solid circles, respectively; other notations and arrow scale here are the same as in Fig. 5. For collinear structure at $N=18$, as well as for $N=24$ in Fig. 7 below, the mean spin deviation from the nominal value $m=\pm 1$ does not exceed 4×10^{-5}. For adjacent values of N, deviation from the $m=\pm 1$ is not small, namely, $m\approx -0.75$ in the corners of the soliton with $N=17$ and $m\approx 0.6$ in the center of a wall segment at $N=19$.

contains a region where all spins have $m=-1$. The region is separated from the rest of the magnet, where $m=+1$, by segments of such walls. This leads us to such spin configuration for which this region would be of the form of a rectangle with the size $l_x \times l_y$, where l_x and l_y are integers. Apparently, the most preferable would be square areas with the spin number l^2 and the magnon number $N=2l^2$. Following Ref. 33, let us call these preferable states "magic." Solitons with $N=N_{\text{magic}}$ have the symmetry axis C_4 (hereunder we discuss the symmetry axis perpendicular to the lattice plane), and the spacious symmetry of a soliton coincides with the lattice symmetry.

Along with magic numbers of magnons $N_{\text{magic}}=2l^2$, "half-magic" states with a rectangle of spins in which l_x and l_y differ by 1 and $N=N_{\text{half-magic}}=2l(l+1)$ are also important. Their symmetry is lower than that for solitons with $N=N_{\text{magic}}$ and includes only the axis C_2. For values like $N=2l(l+2)$, no peculiarities were found; most likely, they are always close to magic numbers, $l(l+2)=(l+1)^2-1$, and proximity effects to the latter are essential.

Let us explain the character of $\omega(N)$ in a soliton with the value N close to magic number. Configurations with $N<N_{\text{magic}}$ can be obtained by "corner smoothing" of a magic configuration due to wall band inward, and are called "ideal square" (see the example with $N=17$ in Fig. 6). Since this does not require a lot of energy, the frequency in the region $N<N_{\text{magic}}$ is small and faintly depends on N, which corresponds well to our numerical calculation. If it is necessary to increase N up to $N>N_{\text{magic}}$, then the situation is different: a domain wall should move into an unfavorable region of the lattice. An increase of N in the region $N>N_{\text{magic}}$ occurs only due to this not profitable wall sector, and frequency values in this region are quite large. It is important to note that for a purely collinear state $(\theta=0,\pi)$, the change of ϕ does not change the system state, and the frequency value has no sense. Therefore, at the transition of N through $N=N_{\text{magic}}$, the $\omega(N)$ dependence experiences a jump. For this reason, two values obtained as frequency limit at $N=N_{\text{magic}}+\varepsilon$ and $N=N_{\text{magic}}-\varepsilon$ are sketched in Fig. 4. In real calculation, the value $\varepsilon=0.01$ was chosen.

It is worthy to discuss an important problem of soliton symmetry. The numerical analysis showed that in this case $N\geqslant N_{\text{magic}}$, the wall growth occurs only from one soliton side (see, for example, $N=19$ in Fig. 6). Note the essential lowering of the soliton symmetry for such values of N, for which the soliton has no symmetry axis at all. The same regularities take place at the transition through half-magic value; however, at $N<N_{\text{half-magic}}$, the soliton symmetry is lower, and it contains an element of C_2 rather than C_4 (see Fig. 7). Then, by increasing N by values like 2–3, the soliton symmetry is restored. Further, when N reaches the next chosen number (half-magic after magic or vice versa), this cycle reiterates (see Fig. 4, where the positions of magic numbers $N=18$ and 32 and half-magic number $N=24$ are depicted).

In fact, such tendency remains at extremely small values of the ratio K/J up to $K/J=0.1-0.3$, when $r_0 \simeq (0.12-0.23)a \ll a$. Again, at $N=1$ and 2, the soliton's size exceeds a, and the soliton can be described within the continuum approximation. Naturally, at small K/J, solitons are

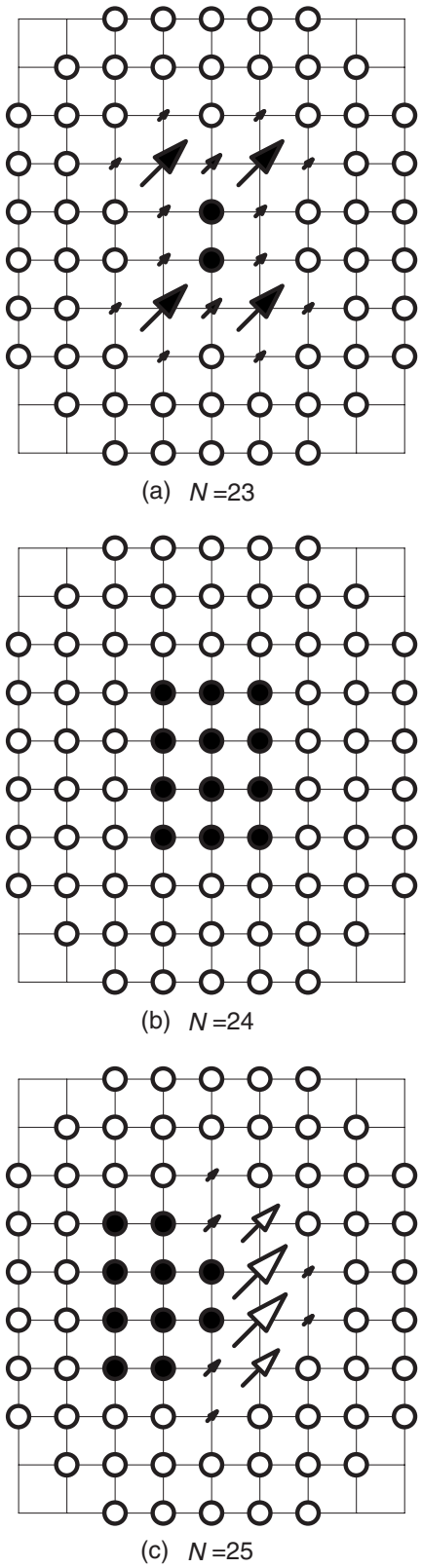

FIG. 7. The distribution of the discrete variables θ_i in a soliton at N close to half-magic value $N=24$. Notations, arrow scale, and the value of $K/J=0.5$ here are the same as in Fig. 6. The value of $m\approx -0.75$ in the corners of the soliton with $N=23$, and $m\approx 0.66$ in the center of a wall segment at $N=25$.

more localized; for example, at $K/J=0.2$, a purely collinear state appears at smaller N like minimal magic number $N=8$. This quantitative difference leads to a qualitatively different feature: at values of $K<K_{(\mathrm{crit})}\simeq 0.36J$ even the states with $N=1$ are localized. These localized states resemble polarons, which are one-electron states localized due to interaction with nonlinear media, see, for example, Ref. 10. These self-localized spin states with $N=1$ can be called *spin polarons*. It is clear that the detailed description of such states with small N should be based on exact quantum analysis, but we believe that our semiclassical consideration gives at least a qualitative estimate for energies of such states. For such small $K<K_{(\mathrm{crit})}\ll J$, the maximal amplitude $\theta(0)$ is not small, the asymptotical solution (20) is not valid any-more, and the energy of spin polaron state $E^{\mathrm{sp}}\equiv E^{(\mathrm{min})}$ is smaller than the continual result $8(J-K)$. The value of spin polaron energy is equal to $2.57J$ at the largest available value of $K=K_{(\mathrm{crit})}\simeq 0.36J$, and grows up to $3.7J$ at $K\ll K_{(\mathrm{crit})}$.

V. RESULT DISCUSSION AND CONCLUDING REMARKS

We considered spin dynamics in non-Heisenberg magnets with the spin $S=1$ and biquadratic exchange taken into account. For such magnets, there are specific longitudinal magnetic solitons, in the center of which the length of magnetization $\langle S_z\rangle$ is smaller than the nominal value $\langle S_z\rangle=1$, the values of $\langle S_x\rangle$ and $\langle S_y\rangle$ are equal to zero, but the oscillations of quadrupolar variables $\langle S_xS_y+S_yS_x\rangle$ and $\langle S_y^2-S_x^2\rangle$ are presented. The energy of such solitons is smaller than that of standard solitons described within the Landau-Lifshitz equation. In particular, this energy is smaller than that for a "transversal" Belavin-Polyakov soliton, for which $|\langle \mathbf{S}\rangle|=1$ and $E_{BP}=4\pi J$. Note that the Belavin-Polyakov soliton as well as other transversal soliton states are also presented in model (1).

Numerical analysis of the discrete lattice model demonstrated the applicability of macroscopic approximation in the vicinity of the SU(3) point, where $J-K\ll J$. For the rest region of parameters, this approximation is adequate for a quantitative (at small N) or semiquantitative, in the general case, description of basic characteristics of solitons, for example, the dependence $E(N)$. The analysis of the discrete model has also demonstrated a series of qualitatively different effects, specifically important when N is large enough and close to some chosen values of the magnon number, magic $N_{\mathrm{magic}}=2l^2$ and half-magic $N_{\mathrm{half\text{-}magic}}=2l(l+1)$, where l is an integer. For these chosen values, a collinear state of solitons is realized, where the magnetization in all points has maximal values $m=\pm 1$.

This result has been obtained within the semiclassical approximation. We were not able to construct such states within exact quantum analysis of model (1). Let us discuss the role of quantum effects. An important question is whether or not the planar solution survives beyond semiclassical approximation. This problem can be discussed by taking into account the presence of usual ferromagnetic gapless transversal magnons within perturbation theory. The existence of an exact semiclassical planar solution means that the equa-

tions for transversal variables, linearized over the planar soliton, have zero solution. In terms of magnons, this means that processes of single magnon radiation described by perturbation Hamiltonian $H_{int}^{(1)}=\Sigma_k[\Psi_{\mathbf{p}}^{(1)}a_{\mathbf{p}}^{\dagger}\exp(i\omega t)+\text{H.c.}]$ are absent [hereupon $a_{\mathbf{p}}$ and $a_{\mathbf{p}}^{\dagger}$ are creation and annihilation operators for such magnons, with linear momentum $\mathbf{p}$ and energy $\varepsilon(\mathbf{p})\simeq J(ap/\hbar)^2$]. In principle, there is a possibility for processes with radiation of several magnons, for example, two-magnon process described by $H_{int}^{(2)}=\Sigma_{1,2}[\Psi_{1,2}^{(2)}a_1^{\dagger}a_2^{\dagger}\exp(i\omega t)+\text{H.c.})$, where $1\equiv\mathbf{p}_1$; three-magnon process, etc. Conservation laws of energy, momentum, and total z projection of spin, which can be written as $E(N)-E(N-2)=\varepsilon(\mathbf{p})+\varepsilon(-\mathbf{p})$, allow this process even at small $E(N)-E(N-2)\simeq 2\hbar\omega\ll J$, as the magnon dispersion law $\varepsilon(\mathbf{p})$ has no gap. One can expect the process of decay from a soliton to magnons due to such radiations of magnons. As a result, the soliton will be characterized by a finite lifetime. Such effects have been discussed early while going beyond the scope of semiclassical approximation for various topological solitons, 2D soliton with nonzero Pontryagin index,[35] and 3D soliton characterized by nonzero Hopf index.[36] However, for aforementioned examples, these processes are slow and the lifetime of a soliton with large enough N is long, $\tau\sim(\hbar/J)N^5$ and $\tau\sim(\hbar/J)N^{5/3}$ in Refs. 35 and 36, respectively. Therefore, one can expect that, in our case, with complete consideration of quantum effects, solitons with a large value of N will be enough long-lived excitations. It is worth noting here that if a small easy-axial magnetic anisotropy is taken into account, it leads to an opening of a gap for transversal magnons; in this case, the soliton lifetime will be even longer.[36] Detailed discussion of this problem goes beyond of the scope of this work.

For solitons in the discrete model, one can point out one more interesting quantum effect absent at regular quantization of continual solutions with radial symmetry. For some special numbers of magnons N, the lowering of soliton symmetry C_4 inherent to the square lattice model (1) occurs down to C_2 or even lower (see Figs. 6 and 7). The presence of solitons with symmetry lower than lattice symmetry C_4 means that, in the classical case, there are several (two or four) equivalent states, which differ from each other by orientation in the lattice. In other words, the classical state of the soliton is degenerated (twofold or even fourfold) with regards to the soliton orientation. In the quantum case, there is a possibility for quantum tunneling (underbarrier transitions) between these states. For large N, the transition probability is low and can be calculated using instanton technique.[6,37] As a result, one can expect the splitting of degenerated states, with the creation of doublet or multiplet with four levels and lifting of the symmetry of the soliton to C_4. We plan to return to a detailed discussion of these effects in our future work.

It is obvious that the observation of effects of longitudinal spin dynamics is possible for materials with nonsmall biquadratic spin interaction. Yet Kittel demonstrated that such interaction appears due to interaction of spin system with lattice deformations.[38] For a common reason, other mechanisms such as electric multipole interactions and the Jahn-Teller effect equally result in biquadratic exchange (see, e.g., Ref. 39). There are a lot of such materials widely known, among them there are almost isotropic magnets (see review of Nagaev[10]).

In summary, it is worthy to discuss the possibility of experimental excitation of longitudinal nonlinear spin dynamics in model (1) considered above. For a standard resonant method, two problems come up. First, frequencies of these modes are rather high; second, magnetic field is coupled with dipole variables (magnetization) only and does not influence directly the quadrupolar variables. Both these problems can be solved by usage of ultrashort intensive laser pulse, see, e.g., Refs. 40 and 41, and see Ref. 23 for a review. Usual value of a pulse duration τ can be as short as 100 fs, and frequencies $\omega\geqslant 1/\tau$, being considerably higher than frequencies of regular spin oscillations, can be effectively excited.

The possible role of different variables, dipolar and quadrupolar, can be demonstrated by a simple example. Consider a thick plane—parallel plate of a ferromagnet saturated along its normal (z axis). Let the light pulse propagate along the z axis, with the electric field parallel to the plate surface. The light interaction with dipolar degrees of freedom $m_i=\langle S_i\rangle$ can be described as follows. Due to inverse Faraday effect, a circularly polarized light is equivalent to a pulse of magnetic field parallel to the z axis.[40,41] Linearly polarized light produces twofold anisotropy in the sample's plane.[21] Both scenario are ineffective for a sample saturated along the z axis, and the excitation of the usual transversal spin oscillations (magnons) is absent in this geometry.

In contrast, the quadrupolar variables like $\langle S_iS_j+S_jS_i\rangle$, with $i,j=x,y$, are coupled directly with linearly polarized light. The influence of such light pulse is equivalent to the *direct action* of some pulse of effective magnetic field $\mathbf{H}^Q(t)$ [see Eq. (15)] on the variable $\boldsymbol{\sigma}$ of the form $H^{(int)}=-\mathbf{H}^Q\boldsymbol{\sigma}$. Being directed perpendicularly to the "ground state magnetization," $\boldsymbol{\sigma}=\mathbf{e}_z$, this pulse field effectively excites the oscillations of the x and y components of $\boldsymbol{\sigma}$, that is, the longitudinal spin oscillations considered in this paper. The excitation of nondipolar spin degrees of freedom by use of ultrafast optical pumping was recently observed for magnetic Mott insulator R_2CuO_4.[42]

ACKNOWLEDGMENTS

We are thankful to V. G. Bar'yakhtar, A. K. Kolezhuk, and D. D. Sheka for stimulated discussions. The work is partially supported by Grant No. INTAS-05-1000008-8112 and by the joint grant from the Ministry of Education and Science of Ukraine and Ukrainian State Foundation of Fundamental Research (F25.2/081).

*bivanov@i.com.ua

[1] A. G. Gurevich and G. A. Melkov, *Magnetization Oscillations and Waves* (CRC, New York, 1996).
[2] V. G. Baryakhtar, B. A. Ivanov, and M. V. Chetkin, Sov. Phys. Usp. **28**, 563 (1985); V. G. Baryakhtar, M. V. Chetkin, B. A. Ivanov, and S. N. Gadetskii, *Dynamics of Topological Magnetic Solitons. Experiment and Theory*, Springer Tract in Modern Physics Vol. 139 (Springer-Verlag, Berlin, 1994).
[3] A. M. Kosevich, B. A. Ivanov, and A. S. Kovalev, Phys. Rep. **194**, 117 (1990).
[4] H.-J. Mikeska and M. Steiner, Adv. Phys. **40**, 191 (1991).
[5] V. G. Bar'yakhtar and B. A. Ivanov, Sov. Sci. Rev., Sect. A **16**, 1 (1992).
[6] B. A. Ivanov, Low Temp. Phys. **31**, 635 (2005).
[7] A. I. Akhiezer, V. G. Bar'yakhtar, and S. V. Peletminskii, *Spin Waves* (North-Holland, Amsterdam, 1968).
[8] H. H. Chen and P. M. Levy, Phys. Rev. Lett. **27**, 1383 (1971); Phys. Rev. B **7**, 4267 (1973).
[9] V. M. Matveev, Sov. Phys. JETP **38**, 813 (1974); Sov. Phys. Solid State **16**, 1067 (1974).
[10] É L. Nagaev, Sov. Phys. Usp. **25**, 31 (1982); *Magnets with Nonsimple Exchange Interactions* (Nauka, Moscow, 1988) (in Russian).
[11] V. M. Loktev and V. S. Ostrovskiĭ, Low Temp. Phys. **20**, 775 (1994).
[12] B. A. Ivanov and A. K. Kolezhuk, Phys. Rev. B **68**, 052401 (2003).
[13] K. Buchta, G. Fáth, Ö. Legeza, and J. Sólyom, Phys. Rev. B **72**, 054433 (2005).
[14] Y. Xian, J. Phys.: Condens. Matter **5**, 7489 (1993).
[15] Zhou Fei, arXiv:cond-mat/0108473 (unpublished).
[16] A. M. Perelomov, Sov. Phys. Usp. **20**, 703 (1977); *Generalized Coherent States and Their Applications* (Springer-Verlag, Berlin, 1986).
[17] E. Fradkin, *Field Theories of Condensed Matter Systems*, Frontiers in Physics Vol. 82 (Addison-Wesley, Reading, MA, 1991).
[18] E. Beaurepaire, J.-C. Merle, A. Daunois, and J.-Y. Bigot, Phys. Rev. Lett. **76**, 4250 (1996).
[19] A. Scholl, L. Baumgarten, R. Jacquemin, and W. Eberhardt, Phys. Rev. Lett. **79**, 5146 (1997).
[20] J. Hohlfeld, E. Matthias, R. Knorren, and K. H. Bennemann, Phys. Rev. Lett. **78**, 4861 (1997).
[21] F. Hansteen, A. V. Kimel, A. Kirilyuk, and Th. Rasing, Phys. Rev. Lett. **95**, 047402 (2005).
[22] C. D. Stanciu, F. Hansteen, A. V. Kimel, A. Kirilyuk, A. Tsukamoto, A. Itoh, and Th. Rasing, Phys. Rev. Lett. **99**, 047601 (2007).
[23] A. V. Kimel, A. Kirilyuk, F. Hansteen, R. V. Pisarev, and Th. Rasing, J. Phys.: Condens. Matter **19**, 043201 (2007).
[24] B. A. Ivanov and R. S. Khymyn, JETP **104**, 307 (2007).
[25] B. A. Ivanov, JETP Lett. **84**, 84 (2006).
[26] N. A. Mikushina, A. S. Moskvin, Phys. Lett. A **302**, 8 (2002).
[27] N. Papanicolaou, Nucl. Phys. B **305**, 367 (1988).
[28] G. B. Whitham, *Linear and Nonlinear Waves* (Wiley-Interscience, New York, 1974).
[29] L. D. Landau and E. M. Lifshitz, *Electrodynamics of Continuous Media*, 1st ed. (Pergamon, Oxford, 1960).
[30] E. A. Turov, A. V. Kolchanov, V. V. Menshenin, I. F. Mirsaev, V. V. Nikolaev, *Symmetry and Physical Properties of Antiferromagnets* (Fizmatlit, Moscow, 2001) (in Russian).
[31] A. K. Zvezdin and V. A. Kotov, *Modern Magneto-Optics and Magneto-Optical Materials* (IoP, Bristol, 1997).
[32] B. A. Ivanov, C. E. Zaspel, and I. A. Yastremsky, Phys. Rev. B **63**, 134413 (2001).
[33] B. A. Ivanov, A. Yu. Merkulov, V. A. Stephanovich, and C. E. Zaspel, Phys. Rev. B **74**, 224422 (2006).
[34] I. G. Gochev, Sov. Phys. JETP **58**, 115 (1983).
[35] B. A. Ivanov, D. D. Sheka, V. V. Krivonos, and F. G. Mertens, Phys. Rev. B **75**, 132401 (2007).
[36] I. E. Dzyaloshinskii and B. A. Ivanov, JETP Lett. **29**, 592 (1979).
[37] E. M. Chudnovsky and J. Tejada, *Macroscopic Quantum Tunneling of the Magnetic Moment* (Cambridge University Press, Cambridge, England, 1998).
[38] C. Kittel, Phys. Rev. **120**, 335 (1964).
[39] P. M. Levy, in *Magnetism in Metals and Metallic Compounds*, edited by J. T. Lopuszanski, A. Pekalski, and J. Przystawa (Plenum, New York, 1976).
[40] A. V. Kimel, A. Kirilyuk, A. Tsvetkov, R. V. Pisarev, and Th. Rasing, Nature (London) **429**, 850 (2004).
[41] A. V. Kimel, A. Kirilyuk, P. A. Usachev, R. V. Pisarev, A. M. Balbashov, and Th. Rasing, Nature (London) **435**, 655 (2005).
[42] V. V. Pavlov, R. V. Pisarev, V. N. Gridnev, E. A. Zhukov, D. R. Yakovlev, and M. Bayer, Phys. Rev. Lett. **98**, 047403 (2007).